Contrib Mineral Petrol (2006) 151: 58–70
DOI 10.1007/s00410-005-0045-4

ORIGINAL PAPER

D.J. Morgan · S. Blake

Magmatic residence times of zoned phenocrysts: introduction and application of the binary element diffusion modelling (BEDM) technique

Received: 17 February 2005 / Accepted: 19 October 2005 / Published online: 30 November 2005

Abstract This paper describes a general technique, binary element diffusion modelling (BEDM), for determining single-crystal residence times in magmas that relies on modelling the diffusion of two or more elements in the crystal. BEDM has the advantage over other diffusion-based models in that it does not need a precisely defined initial compositional profile for the crystal at "zero time", and instead requires that the concentrations of the two elements are correlated during crystallisation. Any differences subsequently observed between the two elements are caused by intracrystalline diffusion during residence in hot magma. These differences are removed by artificially ageing the slower-diffusing of the two elements, and the amount of time taken to "undo" the difference between the elements is simply related to the crystal residence time (=decoupling time) at high temperatures. The BEDM principle is demonstrated using artificial data and is then applied to literature data for Sr and Ba in a zoned sanidine crystal from the Bishop Tuff (Anderson et al., in J. Petrol 41(3):449–473, 2000). For this crystal, the method gives a residence time estimate of 114 ka at 800°C, which is then compared with estimates from other methods. In theory, the method can be further expanded for use as a geothermometer as well as geochronometer. However, this is not easily possible with the diffusivity data currently available.

Communicated by I. Parsons

D.J. Morgan · S. Blake
Department of Earth Sciences, The Open University,
Walton Hall, MK7 6AA Milton Keynes, UK

D.J. Morgan (✉)
Department of Earth Sciences, University of Durham,
Science Laboratories, South Road, DH1 3LE Durham, UK
E-mail: daniel.morgan@durham.ac.uk
Tel.: +44-191-3342329
Fax: +44-191-3342301

Introduction

Phenocrysts record a wealth of information, both compositional and chronological. That historical information can be obtained via isotopic means, for example U series (Condomines et al. 1988; Cooper et al. 2001; Hawkesworth et al. 2000) and Rb–Sr dating (Davies and Halliday 1998), or via diffusional modelling (Costa and Chakraborty 2004; Costa et al. 2003; Davidson et al. 2001; Zellmer et al. 1999). U series work in particular has suffered from the need to analyse an aggregate of a large number of crystals in order to attain the required sample mass for analysis. Given the complex history of many individual crystals, with possible inherited cores and different evolution paths, inclusions and the presence of xenocrysts, such an aggregate will provide an average answer whose significance does not reflect all components that make up the crystal population, and inevitably some information will be obscured as a result. Diffusional models, by contrast, examine single events in single crystals, and allow that complex detail to be investigated. The models rely on the smearing out of compositional variations within crystals by diffusional migration of atoms within the crystal during time spent at magmatic temperature. When the magma cools upon eruption, diffusion slows down by many orders of magnitude, and effectively ceases. This locks information concerning short timescale processes into crystals at eruption time. This information becomes inaccessible by short-lived radio-isotopic methods over geological timescales. If no significant reheating occurs, the diffusional information remains. This provides the potential to retrieve estimates of crystal residence times from igneous rocks regardless of their absolute age. In principle, the residence time can be calculated from the compositional profile and knowledge of the diffusivity of the element in question within that mineral.

As analytical techniques improve in spatial and compositional resolution, diffusion-based models for determining crystal residence times at magmatic

temperatures are becoming more frequently used (Anderson et al. 2000; Coombs et al. 2000; Costa and Chakraborty 2004; Costa et al. 2003; Davidson et al. 2001; Humler and Whitechurch 1988; Morgan et al. 2004; Nakamura 1995; Zellmer et al. 1999). Diffusional methods by nature allow determination of chronologies for single crystals, and this power to analyse individuals or sets of individuals within a large crystal population can tell us much about the homogeneity (or otherwise) of crystal populations (Morgan et al. 2004).

The drawbacks that have to be overcome before diffusional models can be applied include the necessity for very well-constrained geothermometry and the relative scarcity of reliable diffusion coefficients for natural geological materials (Freer 1981). Furthermore, previous models have also relied upon a known or assumed initial state for the crystal under analysis, something that is not always possible to constrain (Anderson et al. 2000; Davidson et al. 2001; Morgan et al. 2004; Zellmer et al. 1999). This paper introduces a methodology for determining the magmatic residence time from two or more trace element traverses in zoned phenocrysts, without the need for an initial assumption of the compositional profile. The method is described in detail in "Theory and methodology", and a worked example is given under "Sources of uncertainty". In the section "Worked example of BEDM" the method is applied to a sanidine phenocryst from the Bishop Tuff.

Theory and methodology

Theory

For the purpose of describing the technique, we shall refer to three types of crystal zonation: abrupt changes in trace element content; changes due to gradual magma mixing; and changes due to gradual melt evolution.

Abrupt discontinuities in crystal zonation are a relatively common phenomenon in volcanic rocks (Dobosi 1989; Ginibre et al. 2002; Shore and Fowler 1996; Simonetti et al. 1996). For the purpose of diffusional analysis of profiles across such discontinuities, an initial state is usually assumed for the compositional profile, (e.g., Zellmer et al. 1999). It is by no means certain that this is justified. By means of a different approach, it is possible to assume that the concentrations of two (or more) trace elements were related during crystallisation of the regions on each side of the discontinuity, and that any divergence from this relationship seen in an analysed crystal is due to the post-crystallisation modification of the concentration profiles by diffusion. This process is likely to occur because elements of differing ionic charge and ionic radius often have marked differences in intracrystalline diffusivity (Freer 1981). The divergence from the relationship will effectively be caused by diffusion causing a mixing between the different regions. If diffusion is faster for one element, then the mixing influence extends further from the initial discontinuity (Fig. 1a, b).

The discontinuity does not necessarily have to be abrupt initially. Indeed, if there is significant variation in trace element content within the crystal, a discontinuity is not necessary, as might be the case if the crystal grew during continued magma mixing. In this case, the zonation can be tackled in one of two ways. If the growth time is short relative to the residence time, then the crystal can be modelled as one zone (Fig. 1c, d). This case can be viewed as a more general version of the abrupt junction case. If the growth continues in bursts over the whole residence history, it should be visible in the trace element zonation, and the crystal can be split into multiple zones for the determination of multiple

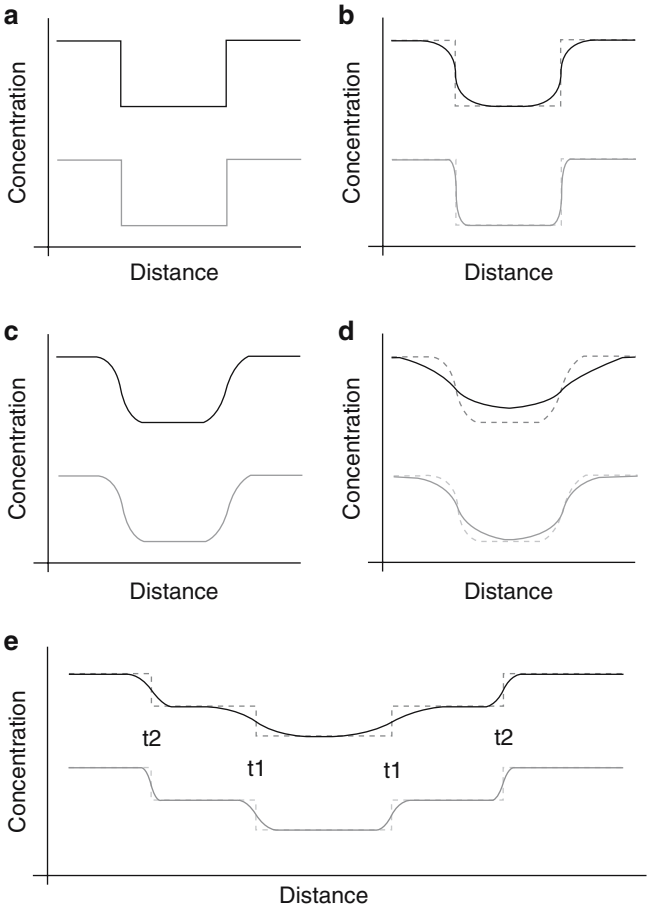

Fig. 1 Different scenarios for the initial distributions (**a**, **c**) of two trace elements of different diffusivity in zoned phenocrysts and possible diffused distributions (**b**, **d**, **e**). Original distributions shown as *dotted lines*, the upper profile shows the distribution of a fast-diffusing element and the lower profile is that of a slower-diffusing element. **a** simple abrupt junction; **b** Abrupt junction after time at magmatic temperature. Note that the profile of the fast-diffusing element is smoothed out further than the slower-diffusing element. **c** A gradual starting profile is identical in both elements. **d** The same diffusional processes as operated between **a** and **b** cause the profiles of the two elements to separate in the same way. **e** A more complex crystal containing multiple abrupt junctions which formed at different times. The separate junctions evolve independently and each is associated with a different event. Note that the upper profile is more diffuse than the lower trace at any given boundary

timescales from multiple regions. An example is shown in Fig. 1e.

A third possibility is that the changes in trace element content are due to gradual melt evolutionary processes. In this case, the crystal should be regarded as a multiple zone as above, provided the growth is not continuous; but matters are not as straightforward as in the magma mixing case as the relationship between the trace elements at the point of crystallisation is not linear due to Rayleigh fractionation. For elements with relatively similar partitioning behaviour, the relationship is very close to being linear; when partitioning is quite different, the line is a curve and, therefore, the linearity assumption for binary element diffusion modelling (BEDM) does not hold, and the method must be modified.

Factors that could interfere in the above linearity assumption include factors such as disequilibrium partitioning of elements during crystal growth limited by diffusion in the melt. Such circumstances have been discussed in the geological and mathematical literature (Albarède and Bottinga 1972; Magaritz and Hofmann 1978; Smith et al. 1955). This process should only occur in cases where there is a significant boundary layer around the crystal which is convection-free; where growth rates are exceedingly rapid; or where elements diffuse to the crystal very slowly. In most volcanic products, this is unlikely to be the case; although such effects have been noted recently in plutonic samples (Gagnevin et al. 2005). Mixing of very different magmas could also cause problems if separate regions in the crystal each display a separate linear trend, although the BEDM software allows analysis of such regions separately.

Fundamental approach

The fundamental approach of the technique is that we assume a linear correlation between the concentrations of two trace elements in a zoned crystal (this is justified in the section "Partitioning"). Because of differential intracrystalline diffusion, the strength of the elemental correlation tends to weaken as the amount of diffusion (expressed by the product of diffusivity and time elapsed) increases. By accelerating the diffusion of the slower-diffusing element (a forward-modelling process), the correlation can be rebuilt. If the diffusivities of the trace elements are known, then the amount of time required to rebuild the correlation can be used to directly calculate the amount of time that the correlation had to decay, which is in effect, the magmatic residence time of that region of the crystal. We, therefore, call our method BEDM. The process is described in detail in the section "Diffusion".

Partitioning

The fundamental assumption of BEDM is that the concentrations of the two correlated elements within each crystal region were governed by simple partitioning laws and constant partition coefficients during the growth of each crystal region. In this scenario, the amount of each trace element in the crystal can be expressed simply as

$$K_{D_A}[A] = mK_{D_B}[B] + n, \tag{1}$$

where m and n are constants, concentrations of A and B in the melt are denoted by square brackets and $K_{D_{A,B}}$ refers to the partition coefficient of A or B in the crystal. This, basically assumes that no disequilibrium process is affecting either of the trace elements (Albarède and Bottinga 1972; Magaritz and Hofmann 1978), and that the degree of evolution during crystallisation is relatively small. Figure 2 shows an example where two model systems are considered for two elements A and B. The upper line shows that with bulk K_D s into the solid phase of $K_D = 5$ for A and $K_D = 2$ for B and F ranging from 1 to 0.8 (20% fractionation), the curve is effectively linear. The lower case shows marked curvature with $K_D = 20$ for A and $K_D = 5$ for B over the same fractionation range. In order to cope with this effect, the modifications required to the BEDM method are trivial, and an appropriate computer program is available from the corresponding author for cases where extensive melt evolution is the dominant control on trace element zonation.

The relative constancy of partition coefficients is supported by studies of partitioning behaviour in crystals (Blundy and Wood 1994; Botazzi et al. 1999; Green and Pearson 1985; Long 1978; Lu et al. 1992; Wood and Blundy 1997). Partition coefficients are, following the work of Blundy and Wood (1994), a function of pressure, temperature and composition of both melt and crystal, governed by equations of the form:

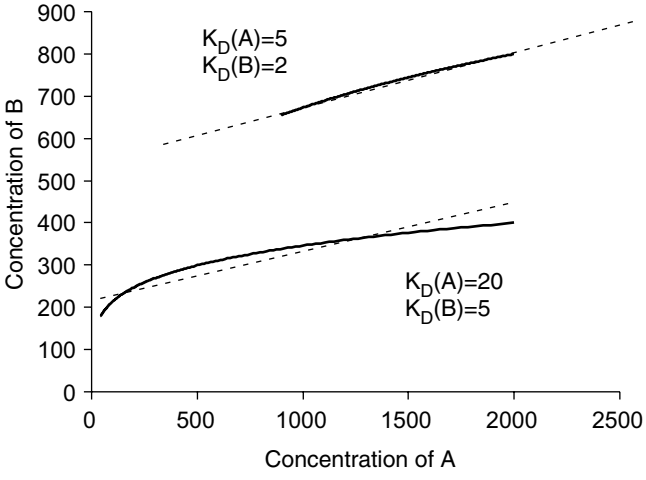

Fig. 2 Graph showing evolution of two elements A and B with different K_Ds into the bulk solid phase with 20% fractional crystallisation. Note that with low and similar K_D s (*upper solid line*) the evolution trend is effectively linear (*dotted line*) with a non-zero intercept. With more extreme K_D s (*lower solid line*) the linear approximation (*dotted line*) is not as strong

$$K_{Di} = A \exp\left(\frac{\Delta G^{y}_{\text{fusion}} - \Delta G^{y-i}_{\text{exchange}}}{RT}\right), \quad (2)$$

where i denotes the partitioning cation and y the "host" cation for that site, R is the gas constant, T is the temperature in Kelvin and A is a constant. In turn, the $\Delta G^{y-i}_{\text{exchange}}$ term can be expressed as the following function:

$$\Delta G^{y-i}_{\text{exchange}} \approx \Delta G_{\text{strain}} = 4\pi E N_{\text{A}}\left[\frac{r_0}{2}(r_i - r_0)^2 + \frac{1}{3}(r_i - r_0)^3\right], \quad (3)$$

where E is the Young's modulus of the cation site, N_{A} is Avogadro's constant, r_0 the ideal site radius and r_i the ionic radius of ion i.

If the pressure, temperature and composition are held constant, the partition coefficients will also be constant. For two isovalent elements such as strontium and barium in alkali feldspar, the behaviour of partition coefficients with respect to varying temperature appear to be very similar (Long 1978); that is to say, the strain energy for exchange would be very similar and the *ratio* of the partition coefficients for the two elements will not vary strongly with temperature. As a result, unless one of the partition coefficients drops below 1, the relative enrichment between elements due to partitioning will be effectively constant, and look identical to paired changes in the overall abundance of those two elements. Variation in pressure may also have an effect, as this can change the ideal ionic radius r_0. Such matters were considered for clinopyroxene by Wood and Blundy (1997), who showed that the pressure dependence is relatively slight. In a subvolcanic system, the pressure changes associated with magmatic movements within the crust should be relatively small in absolute terms. What will have far more effect would be the fluctuations in melt composition and properties caused by the degassing of water and other volatiles. For crystallisation in a stable subvolcanic regime, it is then possible to assume that the partition coefficients for two elements of the same valency in the same crystal of fixed composition are related relatively simply at the point of crystallisation. This appears to work well for sanidine, which in the Bishop Tuff samples has a relatively limited compositional range. For crystals such as plagioclase, the modelling becomes more complex, due to the strong variations in both element partitioning and diffusivity with mineral composition (diffusivity varies by four orders of magnitude between anorthite and albite, for instance Cherniak 1996; Giletti and Casserly 1994). In this case, modelling should be performed with calculated chemical potentials to counteract partitioning effects within the crystal (Costa et al. 2003).

Diffusion

In any diffusing system, the dimensionless parameter Dt/a^2, where D is diffusivity, t is time and a is the spatial scale (point spacing) of the system, represents the amount of diffusion that has occurred. Note that this parameter is not directly analogous to the distance x to which the diffusion front has progressed, as x increases ever more slowly while the rate of diffusion remains constant, governed by the relation $x \propto \sqrt{Dt}$. Ignoring a, which is usually constant, the product Dt, can be thought of as a parameter expressing the absolute amount of diffusion, which at constant temperature increases linearly as a function of time with D as the gradient. If two elements have different values of D, then on a Dt vs. t plot the curves diverge until the crystal is quenched and later analysed (Fig. 3).

The way that BEDM works is that as the gap between the two Dt lines increases with time at magmatic temperature, so the actual trace element distributions become more dissimilar, and so the linear relation between the concentrations of the two elements breaks down. Any analysed crystal can be expected to display some degree of decoupling of its trace elements because the crystal must have spent some time at magmatic temperatures after its initial growth. The two trace elements can be recoupled, however, by artificially "ageing" the traverse for the slower diffusing species, increasing time until the Dt values are the same for both elements (Fig. 2, dotted line). When the correlation between the concentrations of the elements has been re-established, a time of recoupling (t_{rec}) is obtained and the total Dt products for the fast- and slow-diffusing elements are the same. This Dt value can be used to determine the amount of time at magmatic temperature (t_{magma}) that the two elements had to decouple. We call this the magmatic residence time of the crystal, as it is the amount of time spent by the crystal at high temperature in the magma before quenching during eruption. With known diffusivities of D_{f} for the fast-diffusing element and D_{s} for the slow-diffusing element, magmatic residence times can be simply determined as:

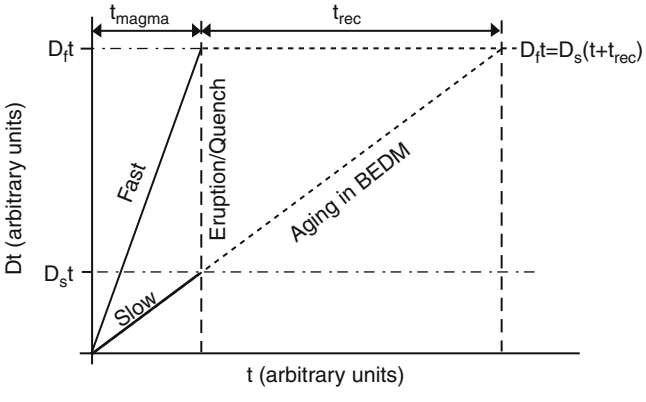

Fig. 3 Schematic Dt versus t plot showing the divergence with time of elements with different values of diffusivity at constant temperature. The quantity of interest is t_{magma}, the magmatic residence time of the phenocryst. This can be estimated from t_{rec}, the recoupling time whereby the slower-diffusing element is re-associated with the faster-diffusing element by modelling further diffusion

$$D_f t_{magma} = D_s\left(t_{magma} + t_{rec}\right), \quad (4)$$

$$t_{magma} = \frac{t_{rec}}{\{(D_f/D_s) - 1\}}. \quad (5)$$

Provided that the assumption of related initial behaviour holds within the analysed crystal region, Eq. 5 will allow a time at magmatic temperature to be determined for that region. This should work for even relatively small differences in relative diffusivity, provided that the trace element measurements show the profile shapes to be clearly different.

From an observed, decoupled, post-eruption profile (e.g. Fig. 1b), the linear relationship can be re-established by artificially modelling the future response of the slower element while leaving the fast-diffusing element in its "erupted" state until the relationship is re-established. The ageing is accomplished by dividing the compositional profile across the crystal into strips which are then allowed to interact according to the one-dimensional diffusion equation (Crank 1975):

$$C = \frac{1}{2} C_0 \left\{ \mathrm{erf}\frac{h - x}{2\sqrt{(Dt)}} + \mathrm{erf}\frac{h + x}{2\sqrt{(Dt)}} \right\}, \quad (6)$$

where C is the composition at point x, h is the half-width of the strip, C_0 the starting composition in the region $-h \leq x \leq +h$, D is the diffusivity and t the time. By integrating over x, the compositional profile can be recalculated for any given time t. The edges of the crystal are assumed to be in equilibrium with the melt, and therefore, are treated as infinite sources.

The time for which the slower element must be "aged" in order to re-couple the two elements, t_{rec}, is then used to calculate the original amount of time over which decoupling occurred, via Eq. 5. However, without knowing a priori how much re-coupling time is needed, the ageing process is an iterative one. In order to solve this, therefore, a computer program (NOVALIS5) was written to perform the ageing of the slower element iteratively. At each time step, the program calculates the distribution of the slow-diffusing element and then tests the correlation between the recalculated concentrations of the slow element and the "erupted" concentrations of the fast element. This is done by fitting a linear regression through the two concentrations and assessing the quality of fit (R^2 value) and the mean size of residual about the line. These two values are used to determine when the best-fit time of recoupling, t_{rec}, has been achieved, and typically give slightly different values, which in turn, yield different values of t_{magma}, called here as R^2 and residual-based age determinations.

Sources of uncertainty

Internal uncertainties

The internal uncertainties in the modelling of the data are a consequence of the size of the data points after interpolation, that is to say, because the analysed 'points' actually have a finite width (or volume, in three dimensions) and the compositional information is averaged over that width, the compositional profile is not smooth, but a step function. This leads to profiles that are on average correct but in detail have atomic populations that are either too far advanced or behind the actual levels (see Fig. 4). These artefacts always cause an underestimate of the true age due to the portions of the profile which are too far advanced with respect to the real distribution. The underestimate is most pronounced when timescales, and hence diffusion distances, are short, relative to the point spacing (i.e. data point width) in the interpolated profile. To express this in terms of the dimensionless "diffusional state" parameter $D_f t/ a^2$ where a is the point spacing, these effects give errors in the ranges shown in Table 1. In all cases with $D_f t/ a^2 > 0.1$ the inaccuracy due to relatively wide points is smaller than those due to the uncertainty in diffusivity (usually a factor of ~2 either way), although this problem does affect the maximum quality of fit (see later). Use of techniques such as BSE imaging (Ginibre et al. 2002; Morgan et al. 2004) to constrain one of the diffusion profiles could increase the spatial resolution, but since BSE imaging portrays the relative atomic number, this will only work for major elements (Mg, Fe in pyroxenes or olivine) or minor elements with relatively large atomic number (Ba in feldspar), and in any case can not be used to constrain more than one of the profiles.

External uncertainties

Measurement uncertainties

In order to test the effect of measurement uncertainties on the BEDM technique, random noise was added to an artificially created data set (see "worked example",

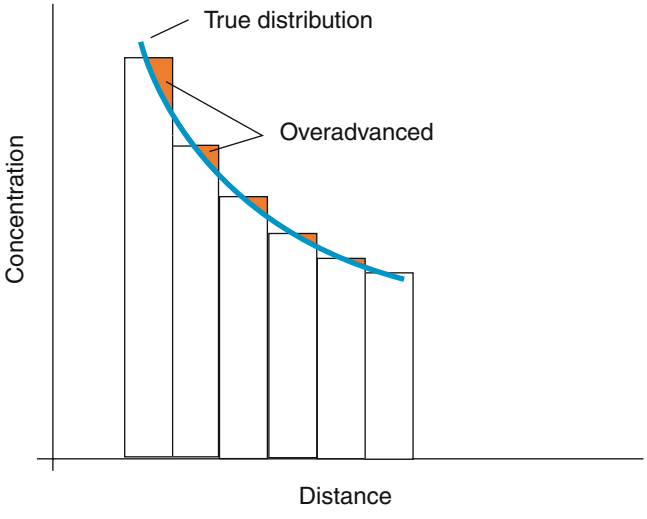

Fig. 4 Generation of errors due to the data point size being large relative to the diffusion length-scale

Table 1 Uncertainties in output age due to width of data points (Internal uncertainties, Fig. 3). These were calculated using artificial datasets decoupled using a standard spreadsheet program and then re-coupled using BEDM

$D_f t/a^2$	Output age relative to actual
0.1	70–100%
1	91–100%
10	96–100%

below). The technique is surprisingly resilient and could take ~6% relative random noise (added after "magmatic decoupling"), far more than found in typical analyses, before breaking down entirely. The effect of adding noise is to cause the R^2 and residual-based age determinations to decouple as the compositional points scatter and this affects the quality of the regression through the data set. The true answer for the data would normally lie between the R^2 and residual answers calculated in the case with noise, even when the noise was as high as 40% relative. However, 6% noise is the point where the behaviour of the output results of R^2 and residual versus calculated/actual age becomes unpredictable and has multiple peaks and troughs. The relatively low impact of random measurement errors is due to the fact that random errors will, on average, cancel out. Thus what should be a re-coupled line, becomes a cloud which, when regressed gives effectively the same line at the same re-coupling time. While the uncertainties will reduce the maximum R^2 obtainable and increase the lowest obtainable residual, they have little influence on the t_{rec} values at which the peak in R^2 and trough in residual occur, if there are a significant number of points and the noise does not dominate the signal.

Diffusivity errors

A variation in one of the diffusivities has an inverse effect on the model times, governed by Eqs. 4 and 5. For instance, if element A diffused 100 times faster than element B, rather than 10 times faster, then the timescales would be 9.9 times smaller, and vice versa. One of the bigger problems is that diffusivities are badly constrained, often with a factor of two or more of uncertainty. This can be overcome by running multiple pairs of similar elements through the model to obtain multiple independent constraints and then combining the results. However, the biggest problem at the moment facing this kind of work is the relative lack of diffusivity data for a wide range of trace elements. Determinations have historically been dominantly concerned with elements relevant to isotopic decay schemes, and matching sets of trace element diffusivities are only now becoming routine. Recent datasets of consistent diffusivity determinations include those for Sr and Ba in feldspar (Cherniak 1996, 2002; Giletti and Casserly 1994); Ni, and Fe–Mg–Mn in olivine (Chakraborty 1997; Dohmen et al. 2003), and the REE in clinopyroxene (Van Orman et al. 2001). Further determinations that would be useful such as Mg and Fe^{2+} in feldspars, or Co, Sc and Cr in clinopyroxenes are yet to be measured as consistent sets. In addition, many known diffusion coefficients are determined at a fixed pressure, oxygen fugacity and usually in the absence of water, meaning that these parameters have unknown effects. Work addressing predictive laws for determining diffusion coefficients (Jaoul and Sautter 1999; Van Orman et al. 2001) has been of some use in extrapolating diffusion behaviour for elements which are currently not constrained but diffusion coefficients determined in this way can not be easily verified.

Temperature errors

As $D = D_0 \exp(-\Delta H/RT)$, there is an inverse exponential dependence of diffusivity on temperature. This means that small errors in the geothermometry propagate into large errors in the diffusional chronometry. As an example, the diffusion rate of strontium in plagioclase increases by a factor of 4.9 between 1,000 and 1,050 K (Giletti and Casserly 1994). For this reason, timescales should be quoted as magmatic ages at a specific temperature, which gives anyone examining the data at a later date an idea of how to treat the timescales given as a function of temperature. This also allows previous data to be recalculated easily should better geothermometry be achieved during later work.

Diffusional effects during crystallisation

There is, in addition to the above, the possibility that diffusional effects in boundary layers around crystals can decouple elements immediately prior to their being incorporated into the crystal (Albarède and Bottinga 1972; Magaritz and Hofmann 1978; Smith et al. 1955). This should only be the case in very cool systems ($T < 700$°C) with large, established and static boundary layers surrounding growing crystals (D.J. Morgan et al., in preparation). In hotter systems, such effects will operate but at length-scales far below that with which this technique is concerned.

Worked example of BEDM

For the purposes of demonstration, an initial set of randomised, artificial data were generated for two hypothetical elements A and B in a crystal at magmatic temperatures. The initial data were generated using the equation

$$[A] = 3[B] + 50 \quad (7)$$

and are used to illustrate the principles of BEDM in Fig. 5a–f. The initial distributions of A and B in the hypothetical crystal at the time of crystallisation are shown in Fig. 5a and the correlation between the elements is shown in Fig. 5b.

These element distributions were then aged through time using a spreadsheet program with $D_A = 10^{-11}$ m^2 s^{-1} and $D_B = 10^{-10}$ m^2 s^{-1} for a time of 1 s with a point spacing of 10^{-6} m; this gives Dt/a^2 for A and B of 10 and 1, respectively. With time, the initial, partition-governed correlation (Eq. 7) progressively breaks down due to differential diffusion of the two elements across the crystal until the crystal is quenched at eruption. This quenched state is represented in Fig. 5c, d, showing the diffused element distributions and their correlation, respectively.

When the elements have been successfully re-coupled, the elemental distributions and correlation look as shown in Fig. 5e, f. Note that the data range of element B has been severely reduced. This corresponds to the same degree of reduction shown by element A in going from Figs. 5a–b to c–d. The two elements have been similarly affected by diffusion and the data ranges reduced correspondingly. However, at this point, the line fitted through the distribution of Fig. 5f should have an R^2 value of 1 and an average absolute per-point difference (residual) between the regressed line and the data points of zero. Incorperating the data from Fig. 5c into the BEDM software, the program gives the results shown in Fig. 6.

Figure 6 shows a distinct R^2 maximum, giving the magmatic age of the crystal as 0.983 s, a discrepancy of 1.7% from the known age. By using the per-point residual instead of R^2, the magmatic age is 0.972 s, a discrepancy of 2.8% from the 1 s diffusion allowed for decoupling. These discrepancies have two main causes. Firstly, the spreadsheet program used to "age" the traverses has for calculation speed reasons quite a coarse point spacing (200 points in x) for determination of the error function distribution (Eq. 6). This is far coarser than the spacing at which the BEDM software calculates the diffusion distribution (up to 640,000 points), and so the spreadsheet suffers from rounding

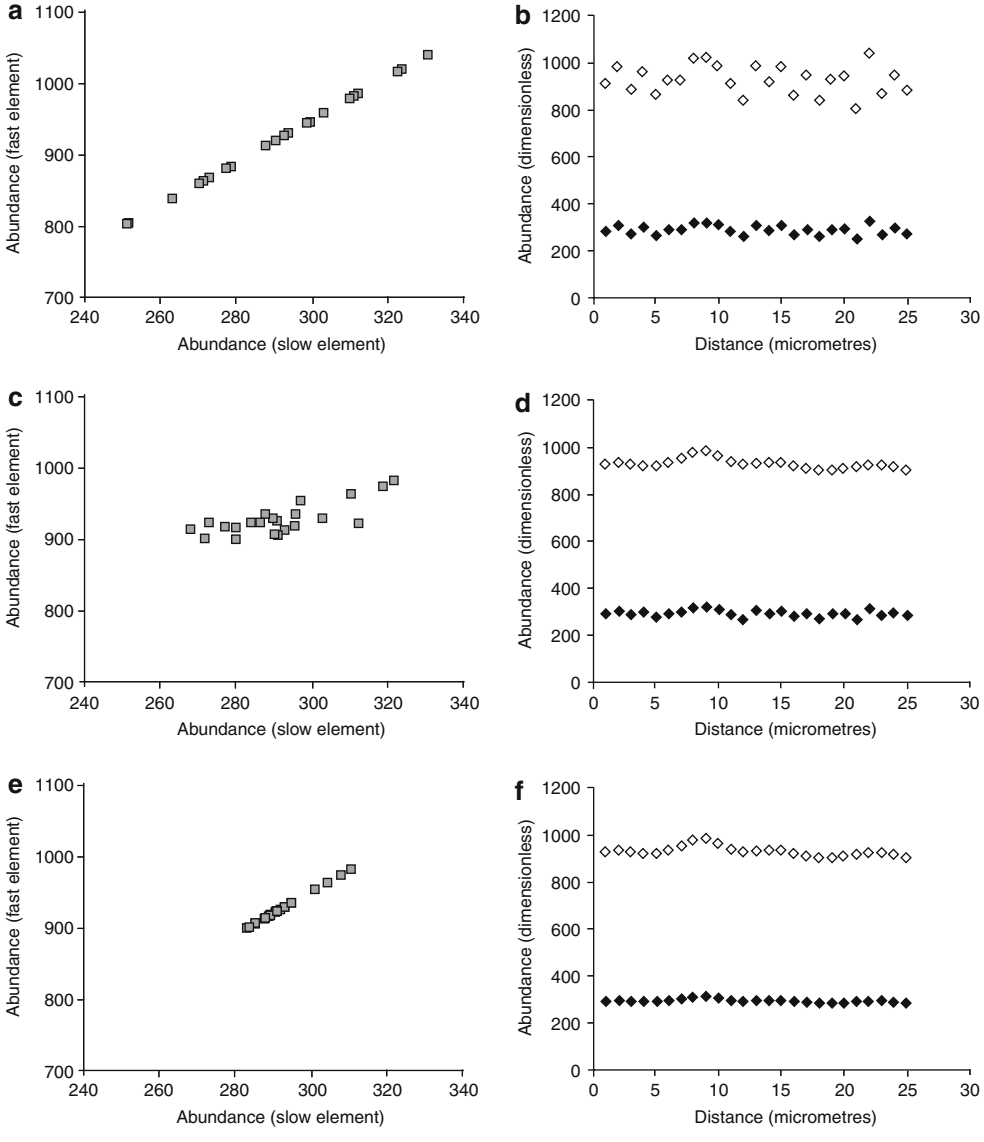

Fig. 5 Distributions of two hypothetical elements in a host crystal. Element A (*hollow diamonds*) diffuses ten times faster than element B (*filled diamonds*). **a** Initially, the concentrations are simply related by the equation $[A] = 3[B] + 50$. **b** The initial zonation in the crystal; the correlation between A and B is as given in (**a**). **c** After one unit of time, diffusion has partly broken down the correlation between A and B, becoming a cloud rather than a line. The range of concentrations of A has been reduced significantly, while that of element B has been reduced to a lesser extent. **d** Diffusion is also seen to have smoothed the compositional profile of A more than the profile of B. **e** The artificial ageing of B has re-coupled the correlation between the two elements, although across a narrower range in composition. **f** After re-coupling, the distribution of B has been smoothed significantly, but the relationship from (**a**) has been regained, albeit at reduced contrast in A and B

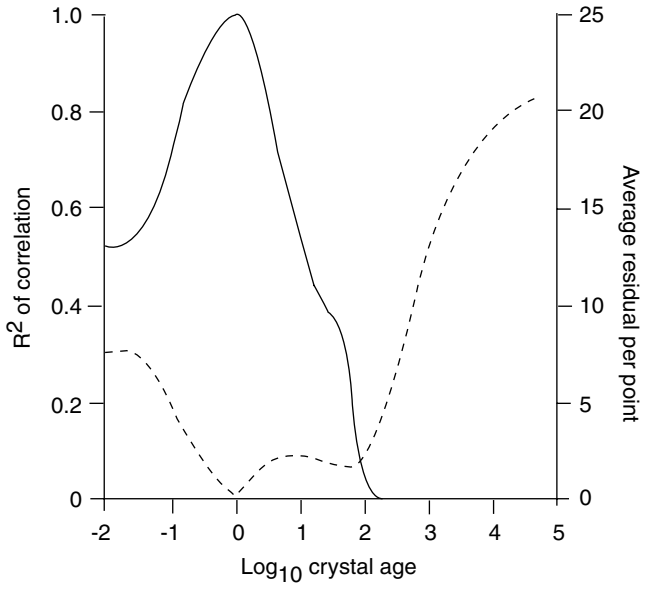

Fig. 6 Results output by BEDM software for the input data of Fig. 5c. Note the strong peak in R^2 and the coincident trough in residual at a time of ~1 time unit

and interpolation errors. Secondly, after being artificially "aged", the concentration profiles of A and B are output as a jagged step function to be input into BEDM. Since the two elements have different extents of diffusion after being aged, this step of reverting to step functions from smooth lines causes additional decorrelation between the elements which is not strictly an effect of diffusion, but an artefact of the binning process. This creates steps in the profile, imposed on the data after the initial decoupling, in areas where the steps had been erased by diffusion. This is exactly the kind of problem referred to in Internal uncertainties section, and Fig. 4, and is an example of what could occur in an actual application; it shows the level of disruption that can be caused by the "binning" of data into points of fixed width.

The same initial data (Fig. 5a,b) were run for several different values of magmatic residence time and the resultant concentration profiles analysed with BEDM. In all cases where the two sides of the crystal were not cross-diffusing (i.e. the diffusion has not removed most contrast), the magmatic residence time corresponding to the peak R^2 value attained was correct to within 10% and frequently better. Comparing the residual and R^2 methods, the residual method usually gave a less accurate estimate of the "actual", or known, residence time than the R^2 method. Discrepancies between the calculated (R^2) and known residence time can usually be ascribed to the width of the data points relative to the size of the traverse. Also, it is worth noting that as magmatic and artificial ageing occur, the compositional contrast of the data set is reduced (compare Fig. 5b and f) and so, there is a smaller region to work with for regression purposes, such that the method becomes less accurate if elements are very strongly homogenised by long periods of diffusion.

To summarise, BEDM, in order to avoid these problems, works best where there is significant diffusion and data points are small and closely spaced, i.e., the parameter $D_f t/a^2$ is greater than 1. This essentially means that the effects of diffusion are spread out across several data points rather than just one or two. Of course, this can go too far; if the diffusion is extreme and covers the entire data set, resolution is lost as there is little compositional contrast across the crystal.

Application of BEDM to sanidine

Sanidine crystals are ideal for applying BEDM as sanidine takes up large amounts of both strontium and barium during crystallisation (Blundy and Wood 1994; Long 1978; Lu et al. 1992), and the diffusion coefficients of both elements are constrained (Cherniak 1996, 2002). Anderson et al. (2000) showed that sanidine from Bishop Tuff rhyolite obeys the main assumption of the BEDM model; that barium and strontium are strongly correlated in the melt, and hence the crystals, at most stages of evolution of the Bishop Tuff. In their paper, Anderson et al. (2000) considered a traverse across a sanidine crystal from the late-erupted Bishop Tuff in terms of diffusive modification of the strontium distribution compared with the distribution predicted from partitioning of barium and strontium between crystal and melt using partition coefficients from Lu et al. (1992). In essence, they considered that the barium distribution represented the un-diffused state and that any deviation from ideal partitioning behaviour seen in the crystal core was due to strontium diffusion. Simply using the length-scale over which that deviation persisted and magmatic temperatures determined by Fe–Ti oxide thermometry (Hildreth 1977, 1979) for the late-stage Bishop Tuff magmas, they estimated a magmatic residence time of between 140 ka and 2.8 Ma. The uncertainty in their estimate is due to uncertainty in the activation energy for Sr diffusion.

In this section, we use their data in a BEDM model as a proof of concept. The traverses published by Anderson et al. (2000) are repeated in Fig. 7. As the crystal is compositionally homogeneous ($Ab_{33–35}$ $Or_{64–66}$ $An_{<1}$, Anderson et al. 2000) and the data display a smooth U-shape, it can be modelled as a single rim-to-rim domain. The fluctuations seen on the left-hand side of the crystal show some barium–strontium anti-correlation, which may be a disequilibrium feature. Due to uncertainty about the origin of this anti-correlation, it has been excluded for the purposes of this study. For analysis, the right-hand side of the traverse was used, and was mirrored about the lowest point to generate the rim-to-rim dataset shown in Fig. 8, which was linearly interpolated at 5-μm intervals for analysis. This was done to remove any of the anti-correlation effects from the left-hand side, and also to remove any possible

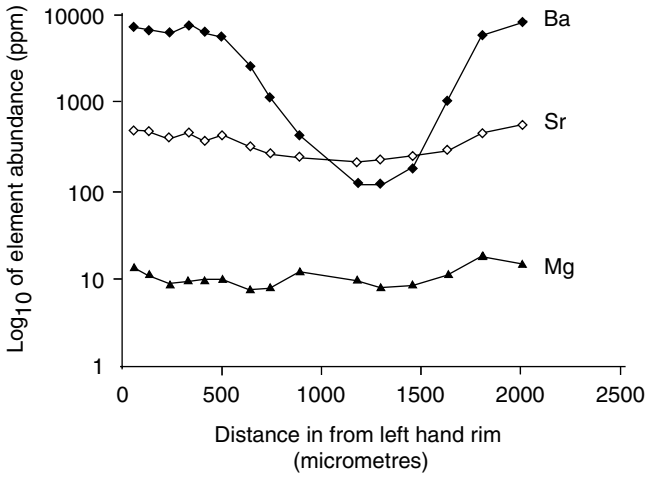

Fig. 7 Selected elemental data taken from the paper of Anderson et al. (2000), for a traverse across sanidine crystal 17A-1 from the Bishop Tuff

effects of asymmetrical sectioning of the crystal (the left side displays a broader profile, implying possibly shallower sectioning). In effect, this process is equivalent to running the right-hand side of the crystal for BEDM, buffering the outside of the crystal against the composition found at the right-hand edge. The mirroring is necessary as both ends of the traverse are considered to be buffered by melt.

Noticeably, the barium profile is a sharper, steeper and wider "U" than the strontium profile, which is considerably shallower. This is because, barium diffuses relatively slowly in sanidine (Cherniak 2002), a consequence of barium ions being larger than strontium ions (Shannon 1976) and as a result causing more lattice deformation during ionic movement.

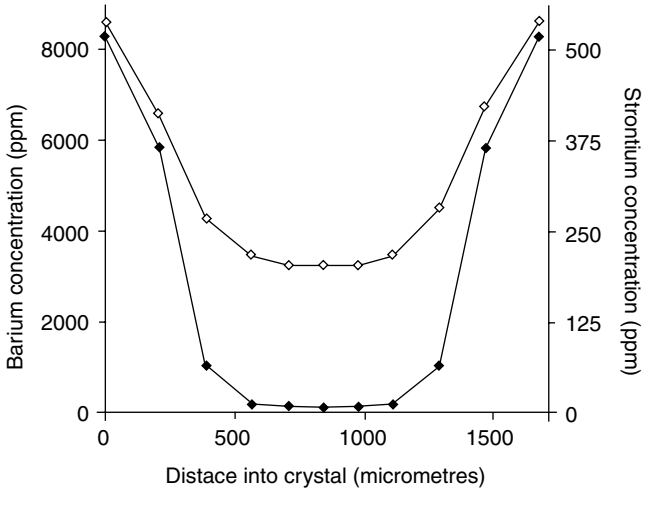

Fig. 8 Barium and strontium data fed to BEDM software. Strontium points are represented by *open diamonds*; *filled diamonds* show barium. Note that the barium curve is much steeper than that of strontium and flatter at the centre, due to the lower diffusivity of barium

Diffusivities were taken from (Cherniak 1996, 2002) and the values of 3.99×10^{-22} m^2 s^{-1} for strontium and 7.73×10^{-24} m^2 s^{-1} for barium were calculated at a temperature of 780°C, the highest temperature measured from the oxide geothermometry of (Hildreth 1977, 1979). For this temperature and ratio of diffusivities, BEDM returns a magmatic residence time between 238 ka by R^2 and 319 ka by residual (Fig. 9). These values lie within the (admittedly large) range quoted by Anderson et al. (2000), of 140 ka to 2.8 Ma. The range in the BEDM estimates has some uncertainty despite the very high peak R^2 value of 0.997. The high R^2 is to some extent an artefact of the dense interpolation; however, the lowest attained residual of 122 ppm per point would suggest that the interpolation is valid. The relative sparsity of the starting data (before interpolation), compared to the size of the profile, and the relatively large size of the data points is rather a problem in terms of the weaknesses of the model discussed in the "Sources of uncertainty" section. However, the very long length of the traverse and the relative smoothness, both act to reduce the severity of these problems. The diffusional state parameter $D_f t/a^2$ for the data of (Anderson et al. 2000), working from the calculated residence time taken to achieve the maximum R^2, is 0.13; and the expected uncertainty in the residence time is, therefore, no worse than ~20% (see Table 1). Given that the data in Fig. 8 were not actually obtained with the BEDM technique in mind, it is a perfectly reasonable test of the technique with real data. Mathematically speaking, Fig. 9 shows extremely good behaviour of the two elements as regards BEDM — the peak shape generated by the model is close to ideal, when compared to the artificial data case (Fig. 6). This shows the following:

1. Strontium and barium zonation in sanidine from the Bishop Tuff exhibits near ideal behaviour with regard to BEDM.
2. The zonation within the crystals is consistent with abrupt zonation caused by a rapid change in magma composition as a linear relation between strontium and barium works with a high degree of success.

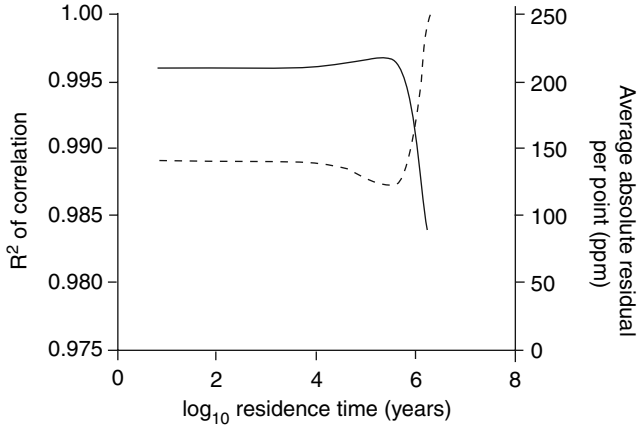

Fig. 9 BEDM output for crystal 17A-1 of Anderson et al. (2000)

3. BEDM determines magmatic timescale results but without any initial compositional state assumptions other than the known related behaviour of strontium and barium.

The whole crystal can also be modelled as one domain, from left rim to right rim. This modelling suggests a longer timescale of 300 ka by R^2 and 360 ka by residual, which is to be expected considering the broader shape of the left side of the profile. In running the complete profile, the lowest attained per point absolute residual is 160 ppm, which is considerably higher than the case for the right side alone, since the two halves of the traverse give different peak times which do not coincide. We prefer the data from the right side, which, due to the more sharply-defined U-shape, give the minimum possible residence time.

Discussion and implications for the Bishop Tuff system

Comparing BEDM with the diffusional model of Anderson et al. (2000), the timescales determined (given the same temperatures) are of a similar order, and the results are compatible with the observable features of the crystal. However, BEDM achieves this without assuming an initial distribution of strontium or barium, merely that the two distributions were related. The timescale that the model implies for the residence time of the sanidine crystal is consistent with many other published estimates for the residence times of crystals in the Bishop Tuff. Previous estimates include determinations for feldspars and quartz crystals ranging up to 10^5 years (Christensen and DePaolo 1993; Christensen and Halliday 1996) or 10^6 years (Davies and Halliday 1998; van den Bogaard and Schirnick 1995) from rubidium–strontium and argon–argon radio-isotopic dating techniques.

However, in reporting timescale data from diffusional methods, it is necessary to remember that there is a very strong dependence on the temperature. For example, if a temperature of 800°C (Ghiorso and Sack 1991) is used in the BEDM model, the residence times drop to between 114 and 136 ka, a marked reduction in the calculated timescales. Furthermore, Fe–Ti oxide thermometers tend to reset relatively quickly, at rates of the order of weeks to months at magmatic temperatures (Coombs et al. 2000; Hammond and Taylor 1982; Nakamura 1995; Venezky and Rutherford 1999). Therefore, they tend to record the immediate pre-eruptive temperature. When considering the residence times of crystals determined by diffusional means, however, the important temperature is the temperature of crystallisation, as most of the diffusion will occur where the temperature is highest, in an analogous manner to diffusion under the conditions of peak metamorphism (Lasaga 1983; Lasaga and Jiang 1995). The crystallisation temperature has the potential to be considerably higher than the eruption temperature, but is difficult to directly constrain. This work can, therefore, only provide a maximum possible estimate of the residence time with the thermometry and diffusion data available.

The temperatures used with BEDM must, therefore, stand only as a minimum estimate and await the determination of the sanidine crystallisation temperature. In themselves, these Fe–Ti oxide temperatures combined with BEDM can only place a maximum constraint on the residence time *at high temperature* for the Bishop Tuff system. Diffusional geochronometry is limited in that it cannot address low-temperature residence. Should the crystals have been imprisoned in a subsolidus mush, the contribution to diffusion within the crystals would effectively be nil over this time as the temperature is much lower. However, it is entirely possible that should the sanidine have initially crystallised at temperatures higher than 800°C, the residence time at that temperature required to explain the observed diffusion is markedly shorter. Such crystals can then leave the magmatic system for a significant amount of time before being remobilised during eruption. Some example residence times for different *crystallisation* temperatures are given in Table 2.

The issue of a cooling rate during crystallisation is also an important one to consider. For the diffusion of strontium and barium, the presence of a cooling regime from, for example, 850 to 800°C leads to a drastic apparent increase in residence time due to the accelerated diffusion at higher temperatures that are not accounted for by an eruption temperature of 800°C. For example, cooling linearly from 850 to 800°C in 500 units of time generates diffusion equivalent to 202 units of time at 850°C or 1,940 units of time at 800°C. Comparing this with the Bishop Tuff analyses, for a similar cooling behaviour, BEDM will overestimate the true residence time by a factor of 3.9. This would mean real crystal residence times are closer to 30 ka than the determined 114–136 ka. Obviously, this problem of variable temperatures is a difficult one to address but could be tackled through relating the Fe–Ti oxide data with studies of phase petrology of similar systems to bracket the possible start and end points of the temperature path for sanidine crystallisation.

Conclusions

The conclusions of this paper address two topics. Firstly, the BEDM method is presented and shown to be a

Table 2 Residence times for Bishop Tuff sanidine (Fig. 8) as a function of temperature

Sanidine crystallisation temperature (°C)	Residence time by R^2 (ka)	Residence time by residual (ka)
780	238	319
800	114	136
810	56.9	76.3
825	28.8	39.1
850	9.73	13.0

viable technique for the determination of magmatic residence times. Secondly, applied to a sanidine crystal from the Bishop Tuff, it gives a residence time using revised thermometry (Ghiorso and Sack 1991), of 114–136 ka at 800°C. However, in interpreting this timescale in terms of its implications for the Bishop Tuff system, matters are rather more complex. That the thermometry is eruption thermometry and not the more desirable crystallisation thermometry means that the temperature estimates are only minima, and the timescale estimates are therefore only maxima. If the eruption and crystallisation temperatures are significantly different, these maxima may be very far off, as shown in Table 2. Therefore the implications of this study for the Bishop Tuff are limited until the sanidine crystallisation temperatures can be fully defined.

The application of BEDM is not necessarily limited to alkali feldspars, and could be applied in any system where multiple elements have predictable partitioning and well-defined diffusion behaviours. In theory, it could be applied to REE in garnet (Burton et al. 1995; Liu et al. 1992), REE in amphibole (Botazzi et al. 1999; Liu et al. 1992), REE in clinopyroxene (Green and Pearson 1985; Liu et al. 1992; Van Orman et al. 2001; Wood and Blundy 1997) and Fe–Mg, Ni, and Ca in olivine (Chakraborty 1997; Coogan et al. 2005; Costa and Chakraborty 2004; Costa and Dungan 2005; Dohmen et al. 2003; Petry et al. 2004).

Expanding BEDM to encompass these minerals is one of the aims of future work, as is the improvement of the software to include three-dimensional diffusion (Costa and Chakraborty 2004). Also, the diffusion of trace elements could be coupled with the diffusion of isotopes in order to improve our understanding of the interaction of isotopic and diffusional geochronometers, which currently reflect widely differing timescales. This form of cross-checking may lead to insights into what is recorded when crystal growth timescales are comparable to the half-lives of the isotopes under examination. This problem is possibly quite common in U-series disequilibrium studies (Charlier and Zellmer 2000) and investigation using non-isotopic methods may yield answers to these issues.

BEDM was developed in part to test if an initial compositional profile assumption was necessary at all. The result is a functional algorithm that avoids such an assumption but which also produces relatively well-constrained magmatic residence times. The current weaknesses in BEDM are the dependence on data of very high spatial resolution and a relative lack of well-determined diffusion coefficients for many elements. However, this last point should be resolved as workers continue to address the issue (Cherniak 2002; Van Orman et al. 2001).

Acknowledgements Fred Anderson, Andy Davis and Louise Thomas are thanked for their kind permission to use their ion-probe data; and the constructive comments from Dr Nick Rogers greatly improved earlier drafts of this manuscript. Constructive and helpful reviews from Daniele Cherniak and Jon Blundy improved the accuracy and clarity of the manuscript. DJM gratefully acknowledges the support of an NERC studentship during the early stages of this work and the later work was supported by ERUPT, EU 5th framework contract number EVG1-CT2002-00058. This paper came about as a result of work presented at the Penrose 2000 conference on the Longevity and Dynamics of Silicic Magma Systems, which the authors both attended.

Appendix

Theoretical extensions to BEDM: multi-element modelling

Should diffusivity data for a wide range of analysable elements become available, BEDM can be expanded to run with multiple pairs of elements for a better set of constraints. Notably, if the diffusivities show different responses to temperature increase, i.e. have different activation energies of diffusion, then it should be possible to use this method to obtain both the residence time and the magmatic temperature of equilibration simultaneously. In order to get strongly different activation energy for diffusion, a difference in ionic charge is often, but not always, necessary. Exceptions exist for minerals such as zircon, where activation energy is a strong function of ionic radius (Cherniak, et al. 1997a, b). It has been noted that site binding energy is essentially a function of ionic charge (Wood and Blundy 1997), and that site binding energy is a primary determinant of the activation energy of diffusion. This leads to the so-called "compensation law" where the lines of log D vs $1/T$ are parallel for ions of the same charge in the same site in the same mineral (Jaoul and Sautter 1999). Therefore, two ions of differing charge will have markedly different responses to temperature, and the ratio of the diffusivities will change as T is varied. In a set of three diffusing ions, if one has a valency different from the other two, running the three possible pairs within the binary element model will only produce the same answer if the temperature is correct and, therefore, the relative diffusivity ratios are also correct. In a graph showing ratios of residence time between element pairs versus temperature of equilibration, this will be the point at which the three lines from each set of modelled ions intersect, shown in Fig. 10.

As it currently stands, this approach will have limited application. Olivine may be a possible starting point (Costa and Dungan 2005), where Ca, Fe–Mg, Ni and Mn diffusion coefficients are known. However, as these authors show, although different elements do give consistent answers and imply the same zonation process (obeying BEDM assumptions), the uncertainties in the diffusion coefficients mean that the timescales are quite different. Therefore, using BEDM in the manner described here with these olivine diffusion coefficients would give quite a wide range in T–time estimates, within uncertainty. In addition, use of

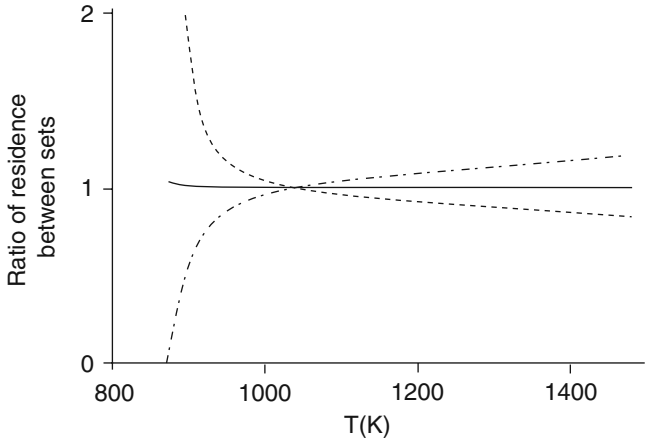

Fig. 10 Simultaneous estimation of temperatures and residence time using BEDM. The magmatic temperature simulated was 1,073K (800°C). The model pins this down precisely at the intersection point of the three lines

BEDM for temperature determinations requires some variation in diffusional activation energy and the listed elements are all quite similar. Therefore, alkali feldspar (for Rb, Sr and Ba diffusion) may be more productive, as these elements sit in the same site in the lattice despite different valency, and have different activation energies.

References

Albarède F, Bottinga Y (1972) Kinetic disequilibrium in trace element partitioning between phenocrysts and host lava. Geochim Cosmochim Acta 36:141–156

Anderson AT, Davis AM, Lu F (2000) Evolution of Bishop Tuff Rhyolitic Magma Based on Melt and Magnetite Inclusions and Zoned Phenocrysts. J Petrol 41(3):449–473

Blundy J, Wood B (1994) Prediction of crystal-melt partition coefficients from elastic moduli. Nature 372:452–454

Botazzi P, Tiepolo M, vannucci R, Zanetti A, Brumm R, Foley SF, Oberti R (1999) Distinct site preferences for heavy and light REE in amphibole and the prediction of $^{Amph/L}D_{REE}$. Contrib Mineral Petrol 137(1–2):36–45

Burton KW, Kohn MJ, Cohen AS, O'Nions RK (1995) The relative diffusion of Pb, Nd, Sr and O in garnet. Earth Planet Sci Lett 133:199–211

Chakraborty S (1997) Rates and mechanisms of Fe–Mg interdiffusion in olivine at 980°C–1300°C. J Geophys Res 102:12317–12331

Charlier B, Zellmer G (2000) Some remarks on U–Th mineral ages from igneous rocks with prolonged crystallisation histories. Earth Planet Sci Lett 183(3–4):457–469

Cherniak DJ (1996) Strontium diffusion in sanidine and albite, and general comments on strontium diffusion in alkali feldspars. Geochim Cosmochim Acta 60(24):5037–5043

Cherniak DJ (2002) Ba diffusion in feldspar. Geochim Cosmochim Acta 66(9):1641–1650

Cherniak DJ, Hanchar JM, Watson EB (1997a) Diffusion of tetravalent cations in zircon. Contrib Mineral Petrol 127:383–390

Cherniak DJ, Hanchar JM, Watson EB (1997b) Rare-earth diffusion in zircon. Chem Geol 134:289–301

Christensen JN, DePaolo DJ (1993) Timescale of large volume silicic magma systems: Sr isotopic systematics of phenocrysts and glass from the Bishop Tuff, Long Valley. Contrib Mineral Petrol 113:100–114

Christensen JN, Halliday AN (1996) Rb–Sr and Nd isotopic compositions of melt inclusions from the Bishop Tuff and the generation of silicic magma. Earth Planet Sci Lett 144:547–561

Condomines M, Hemond C, Allegre CJ (1988) U–Th–Ra radioactive disequilibria and magmatic processes. Earth Planet Sci Lett 90(3):243–262

Coogan LA, Hain A, Stahl S, Chakraborty S (2005) Experimental determination of the diffusion coefficient for calcium in olivine between 900°C and 1500°C. Geochim Cosmochim Acta 69(14):3683–3694

Coombs ML, Eichelberger JC, Rutherford MJ (2000) Magma storage and mixing conditions for the 1953–1974 eruptions of Southwest Trident Volcano, Katmai National Park, Alaska. Contrib Mineral Petrol 140(1):99–118

Cooper KM, Reid MR, Murrell MT, Clague DA (2001) Crystal and magma residence times at Kilauea Volcano, Hawaii: ^{230}Th-^{226}Ra dating of the 1955 east rift eruption. Earth Planet Sci Lett 184(3–4):703–718

Costa F, Chakraborty S (2004) Decadal time gaps between mafic intrusion and silicic eruption obtained from chemical zoning patterns in olivine. Earth Planet Sci Lett 227(3–4):517–530

Costa F, Dungan M (2005) Short time scales of magmatic assimilation from diffusion modeling of multiple elements in olivine. Geology 33(10):837–840

Costa F, Chakraborty S, Dohmen R (2003) Diffusion coupling between trace and major elements and a model for calculation of magma residence times using plagioclase. Geochim Cosmochim Acta 67(12):2189–2200

Crank J (1975) The mathematics of diffusion. Clarendon Press, pp 414

Davidson J, Tepley F III, Palacz Z, Meffan-Main S (2001) Magma recharge, contamination and residence times revealed by in situ laser ablation isotopic analysis of feldspar in volcanic rocks. Earth Planet Sci Lett 184:427–442

Davies GR, Halliday AN (1998) Development of the Long Valley rhyolite magma system: Strontium and neodymium isotope evidence from glasses and individual phenocrysts. Geochim Cosmochim Acta 62(21/22):3561–3574

Dobosi G (1989) Clinopyroxene zoning patterns in the young alkali basalts of Hungary and their petrogenetic significance. Contrib Mineral Petrol 101(1):112–121

Dohmen R, Becker H-W, Chakraborty S (2003) Point defect equilibration and diffusion in olivine at low temperatures ($T <$ 1000°C). Euro J Mineral 15:42

Freer R (1981) Diffusion in silicate minerals and glasses: a data digest and guide to the literature. Contrib Mineral Petrol 76:440–454

Gagnevin D, Daly JS, Poli G, Morgan D (2005) Microchemical and Sr isotopic investigation of zoned K-feldspar megacrysts: insights into the petrogenesis of a plutonic system and disequilibrium processes during crystal growth. J Petrol 46(8):1689–1724

Ghiorso MS, Sack RO (1991) Fe–Ti oxide geothermometry — thermodynamic formulation and the estimation of intensive variables in silicic magmas. Contrib Mineral Petrol 108(4):485–510

Giletti BJ, Casserly JED (1994) Strontium diffusion kinetics in plagioclase feldspars. Geochim Cosmochim Acta 58:3785–3793

Ginibre C, Kronz A, Worner G (2002) High-resolution quantitative imaging of plagioclase composition using accumulated backscattered electron images: new constraints on oscillatory zoning. Contrib Mineral Petrol 142(4):436–448

Green TH, Pearson NJ (1985) Rare earth element partitioning between clinopyroxene and silicate liquid at moderate to high pressure. Contrib Mineral Petrol 91:24–36

Hammond PA, Taylor LA (1982) The ilmenite / titano-magnetite assemblage: kinetics of re-equilibration. Earth Planet Sci Lett 61:143–150

Hawkesworth CJ, Blake S, Evans P, Hughes R, Macdonald R, Thomas LE, Turner SP, Zellmer G (2000) Time scales of crystal fractionation in magma chambers — integrating physical, isotopic and geochemical perspectives. J Petrol 41(7):991–1006

Hildreth EW (1977) The magma chamber of the Bishop Tuff: gradients in temperature, pressure and composition. University of California, Berkeley, pp 328

Hildreth EW (1979) The Bishop Tuff: evidence for the origin of the compositional zonation in silicic magma chambers. Geological Society of America, Special Paper 180:43–76

Humler E, Whitechurch H (1988) Petrology of basalts from the Central Indian Ridge (lat 25°23′S, long 70°04′E): estimates of frequencies and fractional volumes of magma injections in a two-layered reservoir. Earth Planet Sci Lett 88:169–181

Jaoul O, Sautter V (1999) A new approach to geospeedometry based on the "compensation law". Phys Earth Planet Interiors 110:95–114

Lasaga AC (1983) Geospeedometry: an extension of geothermometry. In: Saxena SK (eds) Kinetics and equilibrium in mineral reactions. Springer, Berlin Heidelberg New York, pp 82–114

Lasaga AC, Jiang J (1995) Thermal history of rocks: P–T–t paths from geospeedometry, petrologic data and inverse theory techniques. Am J Sci 295:697–741

Liu C-Q, Masuda A, Shimizu H, Takahashi K, Xie G-H (1992) Evidence for pressure dependence of the peak position in the REE mineral / melt partition patterns of clinopyroxene. Geochim Cosmochim Acta 56:1523–1530

Long PE (1978) Experimental determination of partition coefficients for Rb, Sr, and Ba between alkali feldspar and silicate liquid. Geochim Cosmochim Acta 42:833–846

Lu F, Anderson AT, Davis AM (1992) New and larger sanidine/melt partition coefficients for Ba and Sr as determined by ion microprobe analyses of melt inclusions and their sanidine host crystals. Geological Society of America, Abstracts with Programs 24:A44

Magaritz M, Hofmann AW (1978) Diffusion of Sr, Ba and Na in obsidian. Geochim Cosmochim Acta 42:595–605

Morgan DJ, Blake S, Rogers NW, De Vivo B, Rolandi G, Macdonald R, Hawkesworth CJ (2004) Timescales of crystal residence and magma chamber volume from modelling of diffusion profiles in phenocrysts: Vesuvius 1944. Earth Planet Sci Lett 222(3–4):933–946

Nakamura M (1995) Continuous mixing of crystal mush and replenished magma in the ongoing Unzen eruption. Geology 23(9):807–810

Petry C, Chakraborty S, Palme H (2004) Experimental determination of Ni diffusion coefficients in olivine and their dependence on temperature, composition, oxygen fugacity, and crystallographic orientation. Geochim Cosmochim Acta 68(20):4179–4188

Shannon RD (1976) Revised effective ionic radii and systematic studies of interatomic distances in halides and chalcogenides. Acta Crystallogr A32:751–767

Shore M, Fowler AD (1996) Oscillatory zoning in minerals: a common phenomenon. Can Mineral 34:1111–1126

Simonetti A, Shore M, Bell K (1996) Diopside phenocrysts from nephelinite lavas, Napak volcano, eastern Uganda: evidence for magma mixing. Can Mineral 34(2):411–421

Smith V, Tiller WA, Rutter JW (1955) A mathematical analysis of solute redistribution during solidification. Can J Phys 33:723–744

van den Bogaard P, Schirnick C (1995) $^{40}Ar/^{39}Ar$ laser probe ages of Bishop Tuff quartz phenocrysts substantiate long-lived silicic chamber at Long Valley, United States. Geology 23:759–762

Van Orman JA, Grove TL, Shimizu N (2001) Rare earth element diffusion in diopside: influence of temperature, pressure, and ionic radius, and an elastic model for diffusion in silicates. Contrib Mineral Petrol 141(6):687–703

Venezky DY, Rutherford MJ (1999) Petrology and Fe–Ti oxide re-equilibration of the 1991 Mount Unzen mixed magma. J Volcanol Geother Res 89:213–230

Wood BJ, Blundy JD (1997) A predictive model for rare earth element partitioning between clinopyroxene and anhydrous silicate melt. Contrib Mineral Petrol 129:166–181

Zellmer GF, Blake S, Vance D, Hawkesworth C, Turner S (1999) Short plagioclase residence times at two island arc volcanoes (Kameni islands, Santorini, and Soufriere, St. Vincent) determined by Sr diffusion systematics. Contrib Mineral Petrol 136:345–357